Heriot-Watt University
Research Gateway

Selective Production of Carvacrol from Carvone over Supported Pd Catalysts

Citation for published version:
Benavente, P, Cardenas-Lizana, F & Keane, MA 2017, 'Selective Production of Carvacrol from Carvone over Supported Pd Catalysts', *Catalysis Communications*, vol. 96, pp. 37–40.
https://doi.org/10.1016/j.catcom.2017.03.026

Digital Object Identifier (DOI):
10.1016/j.catcom.2017.03.026

Link:
Link to publication record in Heriot-Watt Research Portal

Document Version:
Peer reviewed version

Published In:
Catalysis Communications

General rights
Copyright for the publications made accessible via Heriot-Watt Research Portal is retained by the author(s) and / or other copyright owners and it is a condition of accessing these publications that users recognise and abide by the legal requirements associated with these rights.

Take down policy
Heriot-Watt University has made every reasonable effort to ensure that the content in Heriot-Watt Research Portal complies with UK legislation. If you believe that the public display of this file breaches copyright please contact open.access@hw.ac.uk providing details, and we will remove access to the work immediately and investigate your claim.

Download date: 05. May. 2023

Selective Production of Carvacrol from Carvone over Supported Pd Catalysts

Pedro Benavente,

Fernando Cárdenas-Lizana* and Mark A. Keane

Chemical Engineering, School of Engineering and Physical Sciences,
Heriot-Watt University, Edinburgh EH14 4AS, Scotland

*corresponding author: tel.: +44(0)131 4514115,
e-mail: F.CardenasLizana @hw.ac.uk

Abstract

The selective conversion of biomass-derived carvone in H_2 was studied over (Al_2O_3, C and CeO_2) supported Pd (mean size 2.8-3.0 nm), taking bulk Pd as benchmark. 100% carvacrol yield was achieved over Pd/Al_2O_3, Pd/C and bulk Pd at an inlet H_2/Carvone = 1/6, with appreciably higher rates for the supported catalysts. Carveol formation over Pd/CeO_2 was attributed to -C=O activation at surface oxygen vacancies (confirmed by O_2 titration) generated during TPR. Carvotanacetone and carvomenthone formation were observed at H_2/Carvone > 1/6.

***Keywords*:** Carvone; carvacrol; hydrogenation; supported Pd.

1 Introduction

Carvone is a terpenoid obtained at low cost by steam distillation of spearmint oil or nitrosochlorination of citrus-derived limonene [1]. Carvone contains three reducible functionalities, a carbonyl group and an endo- and exo-cyclic -CH=CH-. Reaction of carvone with hydrogen generates valuable chemicals (**Figure 1**) in the pharmaceutical, food and agriculture sectors [2]. Reaction selectivity is challenging and most methodologies are non-selective, generating product mixtures [3-6]. Current carvacrol production includes (i) supercritical (300 bar) CO_2 extraction from oregano essential oils [7] and (ii) industrial scale isopropylation of *o*-cresol with propylene over activated alumina at 633 K and 50 bar [8]. The requirements for high operating pressures and temperatures (>523 K) are major drawbacks. Application of supported metal catalysts to promote carvone → carvacrol (in H_2) is an alternative but studies to date are sparse and inconclusive with work focused on batch systems in organic solvents (*e.g.* toluene, hexane, alcohols) [3,6,9-13]. Solvent-free continuous processing at atmospheric pressure offers advantages in terms of throughput and sustainability. The carvone → carvacrol reaction mechanism is still a matter of debate. Klabunovskii *et al.* [13] proposed a classical Horiuti-Polanyi mechanism for reaction over Pd with carvotanacetone as reaction intermediate (**Figure 1**, path **(IA)**). Supported Pt catalysts do not promote carvacrol formation [3,10-12] and selectivities reported for the most selective Pd catalysts [13,14] are low (≤38%).

The redox and acid-base properties of the metal support can influence catalytic activity/selectivity in the reduction of carbonyl and/or unsaturated groups where stronger -C=O (*vs.* -CH=CH-) polarisation on surface Lewis acid sites promotes unsaturated alcohols [15]. Preferential carbonyl and -CH=CH- reduction has been reported over Pd on reducible (CeO_2, TiO_2) [16] and non-reducible (Al_2O_3) oxides [17], respectively. In this study we set out to identify the critical variable(s) that control carvone → carvacrol by examining

commercial and laboratory-synthesised Pd catalysts. We compare the catalytic action of (unsupported) bulk Pd with Pd on (non-reducible Al_2O_3 and reducible CeO_2) oxides and carbon. We evaluate the effect of H_2 content in the feed as a critical process variable.

2 Experimental

2.1 Catalyst Preparation and Activation

Ceria, 1.2% wt. Pd/Al_2O_3, 1.1% wt. Pd/C and PdO were obtained from Sigma-Aldrich. Synthesis of Pd/CeO_2 by deposition-precipitation followed a prior procedure [18]. Samples were sieved to mean diameter = 75 μm, activated in 60 cm^3 min^{-1} H_2 at 10 K min^{-1} to 573 K and passivated in 1% v/v O_2/He at ambient temperature prior to *ex*-situ characterisation.

2.2 Catalyst Characterisation

Palladium content was measured by ICP-OES (Vista-Pro, Varian Inc.). Catalyst activation by temperature programmed reduction (TPR, in 5% v/v H_2/N_2 at 10 K min^{-1} to 573 K), H_2 (at 423 K) and O_2 (at ambient temperature) chemisorption and total specific surface area (SSA, in 30% v/v N_2/He using the single point BET method) measurements were conducted on the commercial CHEM-BET 3000 (Quantachrome) unit as described elsewhere [19]; results were reproducible to ±7%. Palladium particle morphology was determined by scanning transmission electron microscopy (STEM, JEOL 2200FS field emission gun-equipped TEM), employing Gatan Digital Micrograph 1.82 for data acquisition/manipulation. Samples for analysis were crushed and deposited (dry) on a holey carbon/Cu grid (300 Mesh). Surface area-weighted mean Pd sizes (d_{STEM}) were determined from a count of 800 particles [19]. Metal size for bulk Pd was determined by H_2 chemisorption [20].

2.3 Catalytic Procedure

2.3.1 Materials

Carvone (98%), carvacrol (98%), dihydrocarvone (99%) and carveol (98%) were obtained from Sigma-Aldrich. Carvotanacetone, carvomenthone and carvomenthol were synthesised following published methods [21]. All gases (H_2, N_2, O_2 and He) were ultra-high purity (BOC, 99.9%).

2.3.2 Catalytic System

Reactions were conducted at atmospheric pressure and isothermal conditions (423 K) *in situ* after activation in a continuous flow fixed bed vertical tubular glass reactor (15 mm i.d.). A layer of borosilicate glass beads served as preheating zone where the organic reactant was vaporised and reached reaction temperature before contacting the catalyst. Temperature was continuously monitored by a thermocouple inserted in a thermowell within the catalyst bed. The organic reactant was delivered *via* a glass/teflon air-tight syringe and teflon line using a microprocessor controlled infusion pump (Model 100 kd Scientific) at a fixed calibrated flow rate. A co-current flow of N_2, H_2 or H_2+N_2 with carvone (N_2/Carvone = 20/1 mol mol^{-1}, H_2/Carvone = 1/6 – 20/1 mol mol^{-1}) was maintained at gas hourly space velocity (*GHSV*) = 2 × 10^4 – 1 × 10^5 h^{-1}. Palladium (*n*) to reactant (*F*) molar ratio spanned the range 1 × 10^{-5} – 5 × 10^{-2} h. In blank tests, reactions in the absence of catalyst did not result in any measurable conversion. The reactor effluent was frozen in a liquid N_2 trap for analysis using a Perkin-Elmer Auto System XL gas chromatograph with split/splitless injector, FID and Stabilwax capillary column (RESTEK). Data acquisition/manipulation used the TotalChrom data system. Fractional carvone conversion (*X*) is given by:

$$X = \frac{[\text{Carvone}]_{in} - [\text{Carvone}]_{out}}{[\text{Carvone}]_{in}} \quad \textbf{(1)}$$

with selectivity to carvacrol ($S_{Carvacrol}$):

$$S_{\text{Carvacrol}}\ (\%) = \frac{[\text{Carvacrol}]_{\text{out}}}{[\text{Carvone}]_{\text{in}} - [\text{Carvone}]_{\text{out}}} \times 100 \quad \textbf{(2)}$$

and yield ($Y_{\text{Carvacrol}}$):

$$Y_{\text{Carvacrol}}\ (\%) = X \times S_{\text{Carvacrol}} \quad \textbf{(3)}$$

Catalytic activity is also quantified in terms of reactant consumption rate (R, $\text{mol}_{\text{Carvone}}\ \text{mol}_{\text{Pd}}^{-1}\ \text{s}^{-1}$), extracted from time on-stream measurements [22]. Turnover frequency (*TOF*, rate per active site) was determined from particle size measurements [22]. Repeated reactions with different samples from the same batch of catalyst delivered raw data reproducibility and carbon mass balances within ±5%.

3 Results and Discussion

3.1 Catalyst Characterisation

Physicochemical properties of the catalysts in this study are given in **Table 1**. The commercial and laboratory synthesised samples display a range of SSA (3-870 $\text{m}^2\ \text{g}^{-1}$). The TPR profiles (**Figure 2**) exhibit a negative peak (H_2 release) at 350-383 K due to decomposition of Pd hydride formed by H_2 absorption at ambient temperature [20]. The lower hydride Pd/H ratio for supported (0.06-0.04) relative to bulk Pd (0.67) is consistent with nano-scale metal particles as is the shift to lower decomposition temperatures [20]. TPR of Pd/CeO_2 (**Figure 2(IV)**) presents a positive peak at the final isothermal hold (573 K), suggesting partial CeO_2 reduction (at the metal-support interface) with the formation of oxygen vacancies [23]. This was confirmed by O_2 titration post-TPR where O_2 uptake (160 $\mu\text{mol}\ \text{g}^{-1}$) is comparable with values in the literature [24]. Hydrogenation performance is determined by the capacity of Pd for H_2 adsorption/dissociation [20]. Hydrogen chemisorption at reaction temperature (**Table 1**) was close to detection limits for bulk Pd and appreciably lower than that recorded for the supported systems. Uptake was equivalent for Pd/Al_2O_3 and Pd/C and measurably higher for Pd/CeO_2. Differences in H_2 chemisorption can

be due to variations in metal dispersion [19]. The three supported catalysts present pseudo-spherical Pd particles in the 1-6 nm range (**Figure 3(I)**) with a similar size distribution (**Figure 3(II)**) and mean (d_{STEM} ~ 3 nm, **Table 1**). Greater H_2 chemisorption on Pd/CeO_2 can be linked to partial support reduction with the generation of sites for H_2 adsorption. Wang *et al*. [25] have recently discussed the formation of active sites at the interface of metal nanoparticles strongly interacting with reducible CeO_2. Tu and Cheng [26] reported a synergistic effect between Pd and CeO_2 that resulted in stronger H_2 adsorption and increased uptake.

3.2 Gas Phase Conversion of Carvone

Reaction thermodynamics establishes greater stability of conjugated endo-cyclic -CH=CH- and carbonyl functionalities in carvone [27] with the following order of decreasing reactivity based on Gibbs free energy [28]: exo -CH=CH- > endo -CH=CH- > -C=O. This can account for the reported formation of unsaturated and saturated ketones (**Figure 1** (path **(II)**)) as principal products in the hydrogenation of carvone [6]. Variations in H_2 content in the feed (represented as inlet H_2/Carvone) were tested in order to probe reaction pathway. A range of H_2/Carvone ratios was considered, from 0 (reaction in N_2) to sub- (H_2/Carvone = 1/6), stoichiometric (= 1/1) and H_2 in excess (= 20/1) for the reduction of a single carvone functionality. Under all reaction conditions, formation of dihydrocarvone (endo -CH=CH- reduction, path **(III)**) and carvomenthol (-C=O reduction in carvomenthone, path **(II)**) was negligible with selectivities ≤6%.

Reaction in N_2 did not result in any measurable conversion of carvone. Under hydrogen lean conditions (H_2/Carvone = 1/6), we achieved full selectivity to the target carvacrol for reaction over bulk Pd, Pd/Al_2O_3 and Pd/C (**Table 1** and **Figure 4(I)**). This result is significant given the reports in batch liquid phase carvone hydrogenation where low selectivity to carvacrol (≤38%) was obtained over unsupported Pd [13] and (C and Al_2O_3) supported Pd

[13,14]. Variations in contact time can govern selectivity [29] and the exclusivity to carvacrol achieved in this study may result from the lower contact time (0.03-0.2 s) in continuous operation. Negligible conversion of carvotanacetone was recorded for reactions in N_2 or H_2 lean conditions. This indicates direct carvacrol formation from carvone *via* hydrogen migration and keto-enol tautomerisation, following path **(IB)** in **Figure 1**. Catalytic inactivity for carvone reaction in N_2 suggests that carvacrol formation requires H_2 in the feed. This is in line with recent work by Zhang *et al.* [30] who reported formation of phenols over Pd/C *via* hydrogen treatment of substituted 2-cychlohexenones. Naito and Tanimoto [31] provided direct evidence for intramolecular double-bond migration in propene hydrogenation over Pd/SiO_2 while Musolino *et al.* [32] established a hydrogen requirement for double bond migration in *cis*-2-butene-1,4-diol → 2-hydroxytetrahydrofuran transformation over Pd/C.

Pd/CeO_2 exhibited different behaviour in promoting carveol formation (S = 10%) *via* -C=O hydrogenation (path **(IV)** in **Figure 1**). This can be attributed to the involvement of surface oxygen vacancies where the carbonyl group is activated at Ce^{3+} sites for hydrogen attack to generate carveol. Neri *et al.* [16] proposed preferential formation of an unsaturated alcohol from an unsaturated aldehyde over Pd on reducible oxides (TiO_2, ZnO, Fe_2O_3), which they ascribed to reactant activation on the support. Calaza *et al.* [33] demonstrated (by TPD, RAIRS and DFT) carbonyl activation at oxygen vacancies on CeO_2. We observed an initial decline in conversion that attained steady state for all the systems (see inset to **Figure 4(I)** for Pd/Al_2O_3). Similar reaction rates (and *TOF*) were obtained for the three supported Pd catalysts, which were appreciably greater than bulk Pd (**Table 1**) and can be linked to H_2 uptake capacity under reaction conditions. At an inlet H_2/Carvone =1/6, carvacrol yield was proportional to Pd content (**Figure 4(II)**) to reach 100% in the case of Pd, Pd/Al_2O_3 and Pd/C. The lower yield over Pd/CeO_2 was due to carveol formation. An increase in H_2/Carvone resulted in decreased carvacrol selectivity where the data for all the catalysts

converged on a common trend line (**Figure 4(I)**). Loss of carvacrol selectivity with increasing H_2 content was accompanied by formation of carvotanacetone and carvomenthone, which were promoted at higher H_2/Carvone (**Table 1**). Olefin conversion over transition metal catalysts proceeds through an allyl intermediate that is formed by a hydrogen addition [34]. This intermediate can undergo (i) H elimination with bond migration or (ii) insertion of a second H to generate the alkane [34]. The switch from double bond migration (path **(IB)** in **Figure 1**) to hydrogenation (path **(II)**) is sensitive to H_2/Carvone, which is consistent with the literature [32]. Hydrogen elimination is favoured under conditions of low surface hydrogen (H_2/Carvone = 1/6). Increased H_2 content facilitates H insertion, directing the reaction to preferential hydrogenation. Carveol formation over Pd/CeO_2 was insensitive to H_2/Carvone.

4 Conclusions

We have established exclusive formation of carvacrol at full carvone conversion over Pd/Al_2O_3 and Pd/C (mean Pd size = 2.8-3.0 nm) at an inlet H_2/Carvone = 1/6. Under the same reaction conditions, bulk Pd with lower H_2 uptake capacity delivered 100% carvacrol yield at a lower rate. Reaction over Pd/CeO_2 promoted formation of carveol due to -C=O activation at oxygen vacancies created during TPR. Hydrogenation to carvotanacetone and carvomenthone was promoted at higher H_2/Carvone (>1/6).

References

[1] J. L. Bicas, A. P. Dionísio, G. M. Pastore, Chem. Rev. 109 (2009) 4518-4531.

[2] W. Schwab, C. Fuchs, F.-C. Huang, Eur. J. Lipid Sci. Technol. 115 (2013) 3-8.

[3] I. M. J. Vilella, S. R. de Miguel, O. A. Scelza, J. Mol. Catal. A: Chem. 284 (2008) 161-171.

[4] L. J. Lemus-Yegres, M. Pérez-Cadenas, M. C. Román-Martínez, C. S.-M. de Lecea, Micropor. Mesopor. Mater. 139 (2011) 164-172.

[5] V. P. Sivcev, K. P. Volcho, N. P. Salakhutdinov, V. I. Anikeev, J. Supercrit. Fluid. 80 (2013) 9-14.

[6] C. I. Melo, Alternative Solvents in Carvone Hydrogenation, MsC Thesis, E. Bogel-Łukasik, Chemical Engineering, Universidade Nova de Lisboa, Lisbon, 2011, pp. 53.

[7] A. Ocaña-Fuentes, E. Arranz-Gutiérrez, F. J. Señorans, G. Reglero, Food Chem. Toxicol. 48 (2010) 1568-1575.
[8] G. D. Yadav, S. B. Kamble, J. Chem. Technol. Biotechnol. 84 (2009) 1499-1508.
[9] C. I. Melo, R. Bogel-Łukasik, E. Bogel-Łukasik, J. Supercrit. Fluid. 61 (2012) 191-198.
[10] S. R. de Miguel, M. C. Román-Martínez, D. Cazorla-Amorós, E. L. Jablonski, O. A. Scelza, Catal. Today 66 (2001) 289-295.
[11] G. C. Torres, S. D. Ledesma, E. L. Jablonski, S. R. de Miguel, O. A. Scelza, Catal. Today 48 (1999) 65-72.
[12] S. R. de Miguel, M. C. Román-Martínez, E. L. Jablonski, J. L. G. Fierro, D. Cazorla-Amorós, O. A. Scelza, J. Catal. 184 (1999) 514-525.
[13] E. I. Klabunovskii, L. F. Godunova, L. K. Maslova, B. Acad. Sci. USSR Chem. Sci. 21 (1972) 1020-1024.
[14] C. I. Melo, R. Bogel-Łukasik, M. G. da Silva, E. Bogel-Łukasik, Green Chem. 13 (2011) 2825-2830.
[15] S. Handjani, E. Marceau, J. Blanchard, J.-M. Krafft, M. Che, P. Mäki-Arvela, N. Kumar, J. Wärnå, D. Y. Murzin, J. Catal. 282 (2011) 228-236.
[16] G. Neri, G. Rizzo, L. de Luca, A. Donato, M. G. Musolino, R. Pietropaolo, Appl. Catal. A: Gen. 356 (2009) 113-120.
[17] B. C. Campo, M. A. Volpe, C. E. Gigola, Ind. Eng. Chem. Res. 48 (2009) 10234-10239.
[18] N. S. Babu, N. Lingaiah, N. Pasha, J. V. Kumar, P. S. S. Prasad, Catal. Today 141 (2009) 120-124.
[19] M. Li, X. Wang, Y. Hao, F. Cárdenas-Lizana, M. A. Keane, Catal. Today 279 (2017) 19-28.
[20] F. Cárdenas-Lizana, Y. Hao, M. Crespo-Quesada, I. Yuranov, X. Wang, M. A. Keane, L. Kiwi-Minsker, ACS Catal. 3 (2013) 1386-1396.
[21] C. Petrier, J.-L. Luche, Tetrahedron Lett. 28 (1987) 2351-2352.
[22] M. Li, Y. Hao, F. Cárdenas-Lizana, H. H. P. Yiu, M. A. Keane, Top. Catal. 58 (2015) 149-158.
[23] N. C. Nelson, J. S. Manzano, A. D. Sadow, S. H. Overbury, I. I. Slowing, ACS Catal. 5 (2015) 2051-2061.
[24] S. Salasc, V. Perrichon, M. Primet, N. Mouaddib-Moral, J. Catal. 206 (2002) 82-90.
[25] Y.-G. Wang, D. Mei, V.-A. Glezakou, J. Li, R. Rousseau, Nature Commun. 6 (2015) 1-8.
[26] C. Tu, S. Cheng, ACS Sust. Chem. Eng. 2 (2014) 629-636.
[27] R. A. Kjonaas, S. P. Mattingly, J. Chem. Educ. 82 (2005) 1813-1814.
[28] P. Barbaro, F. Liguori, Heterogenized Homogeneous Catalysts for Fine Chemicals Production: Materials and Processes, Springer, Dordrecht, 2010.
[29] Y. Hao, M. Li, F. Cárdenas-Lizana, M. A. Keane, Catal. Lett. 146 (2016) 109-116.
[30] J. Zhang, Q. Jiang, D. Yang, X. Zhao, Y. Dong, R. Liu, Chem. Sci. 6 (2015) 4674-4680.

[31] S. Naito, M. Tanimoto, J. Catal. 102 (1986) 377-385.

[32] M. G. Musolino, C. M. S. Cutrupi, A. Donato, D. Pietropaolo, R. Pietropaolo, Appl. Catal. A: Gen. 243 (2003) 333-346.

[33] F. C. Calaza, Y. Xu, D. R. Mullins, S. H. Overbury, J. Am. Chem. Soc. 134 (2012) 18034-18045.

[34] W. Ludwig, A. Savara, S. Schauermann, Dalton Trans. 39 (2010) 8484-8491.

Table 1: Palladium content, specific surface area (SSA), H_2 chemisorption (at 423 K), mean Pd size (d_{STEM}), carvone consumption rate (R) and turnover frequency (TOF) and carvacrol, carvotanacetone and carvomenthone selectivity ($S_{Product}$) at X ~ 0.3 for different inlet H_2/Carvone.

Catalyst	Pd content (% wt.)	SSA ($m^2\ g^{-1}$)	H_2 uptake (mmol g_{Pd}^{-1})	d_{STEM} (nm)	H_2/Carvone = 1/6		$S_{Carvotanacetone}/S_{Carvomenthone}$ (%)		
					R ($mol_{Carvone}\ mol_{Pd}^{-1}\ s^{-1}$) / TOF (s^{-1})	$S_{Carvacrol}$ (%)	H_2/Carvone		
							1/1	5/1	10/1
Pd	-	3	<0.04	-	1.4×10^{-3} / 0.2[a]	100	30/0	29/13	28/14
Pd/Al_2O_3	1.2	145	1.7	3.0	2.3 / 6.2	100	12/1	15/4	21/8
Pd/C	1.1	870	2.0	2.8	2.3 / 5.7	100	13/1	17/2	27/7
Pd/CeO_2	0.5	37	9.0	3.0	2.5 / 6.7	90	13/0	18/2	24/3

[a]*TOF* obtained using Pd size (=130 nm) from H_2 chemisorption (see Experimental section).

Figure captions

Figure 1: Reaction pathways in the conversion of carvone to (target) carvacrol (**path I**, solid arrows), carvomenthol (**path II**, open arrows), dihydrocarvone (**path III**, dashed arrow) and carveol (**path IV**, dotted arrow).

Figure 2: Temperature programmed reduction (TPR) profiles for **(I)** PdO, **(II)** Pd/Al_2O_3, **(III)** Pd/C and **(IV)** Pd/CeO_2.

Figure 3: (I) Representative STEM image with **(II)** Pd size histogram for **(A)** Pd/Al_2O_3, **(B)** Pd/C and **(C)** Pd/CeO_2.

Figure 4: (I) Effect of inlet H_2/Carvone on selectivity to carvacrol ($S_{Carvacrol}$). *Inset*: variation of carvone fractional conversion (X) with time on-stream over Pd/Al_2O_3 (■); **(II)** variation of carvacrol yield ($Y_{Carvacrol}$) with Pd content in the catalyst bed (n) for reaction over Pd (★), Pd/Al_2O_3 (□), Pd/C (△) and Pd/CeO_2 (○). *Note*: Bottom x-coordinate in **(II)** refers to Pd (★). *Reaction conditions*: T = 423 K, H_2/Carvone = 1/6 – 20/1, $n/F = 1 \times 10^{-5} – 5 \times 10^{-2}$ h, $GHSV = 2 \times 10^4 – 1 \times 10^5$ h^{-1}.

Figure 1

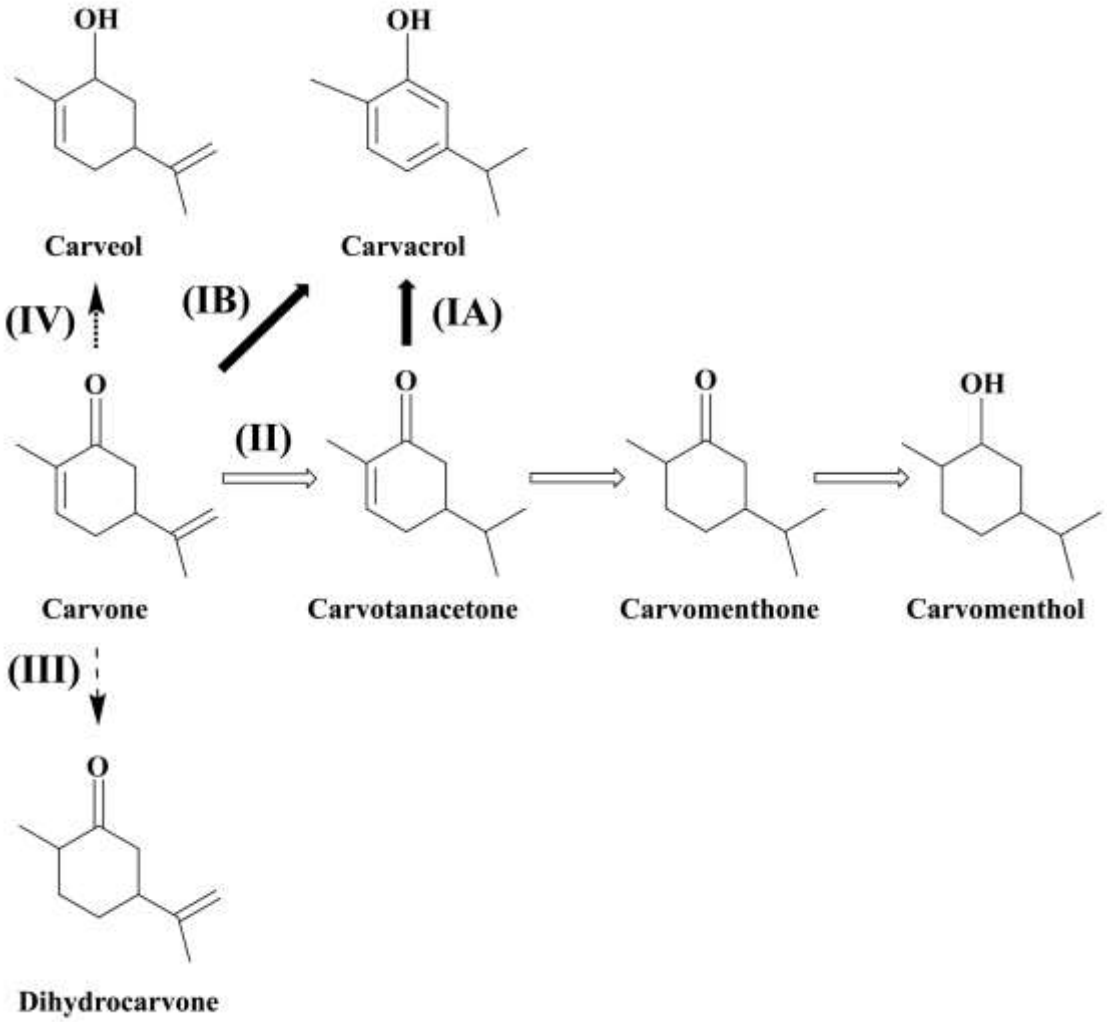
OH
OH
Carveol
Carvacrol
(IV)
(IB)
(IA)
O
O
O
OH
(II)
Carvone
Carvotanacetone
Carvomenthone
Carvomenthol
(III)
O
Dihydrocarvone

Figure 2

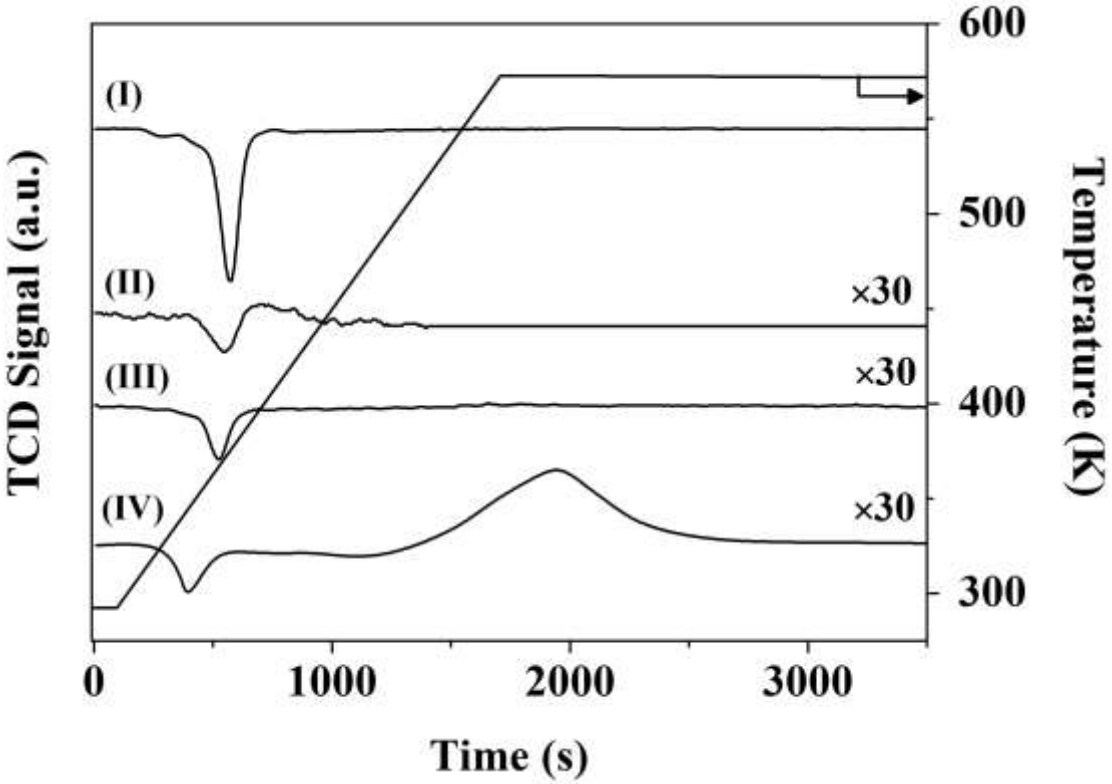
TCD Signal (a.u.)
Temperature (K)
Time (s)
(I)
(II)
(III)
(IV)
×30
×30
×30
600
500
400
300
0
1000
2000
3000

Figure 3

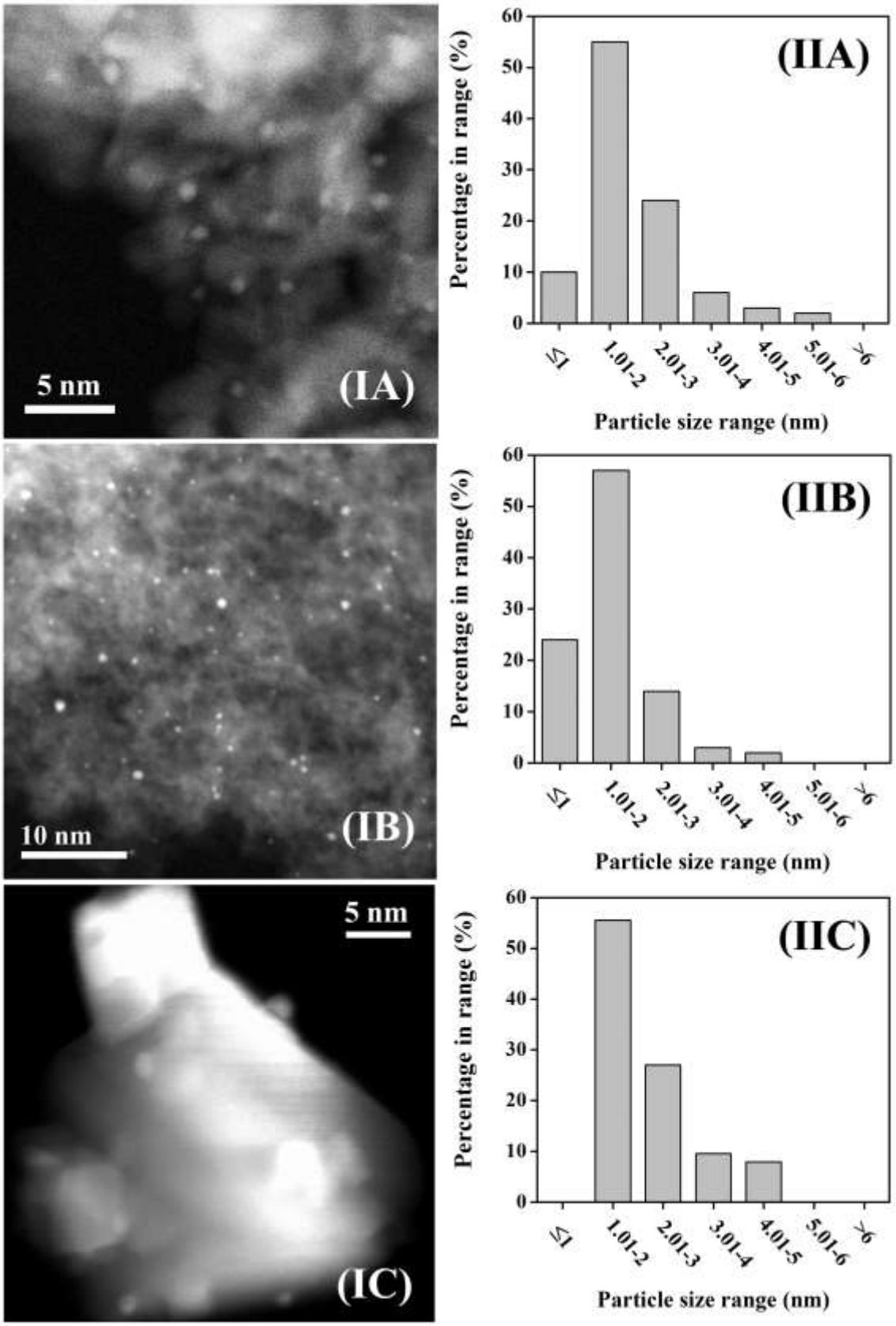
5 nm
(IA)
(IIA)
Percentage in range (%)
Particle size range (nm)
10 nm
(IB)
(IIB)
Percentage in range (%)
Particle size range (nm)
5 nm
(IC)
(IIC)
Percentage in range (%)
Particle size range (nm)
≤1
1.01-2
2.01-3
3.01-4
4.01-5
5.01-6
>6

Figure 4

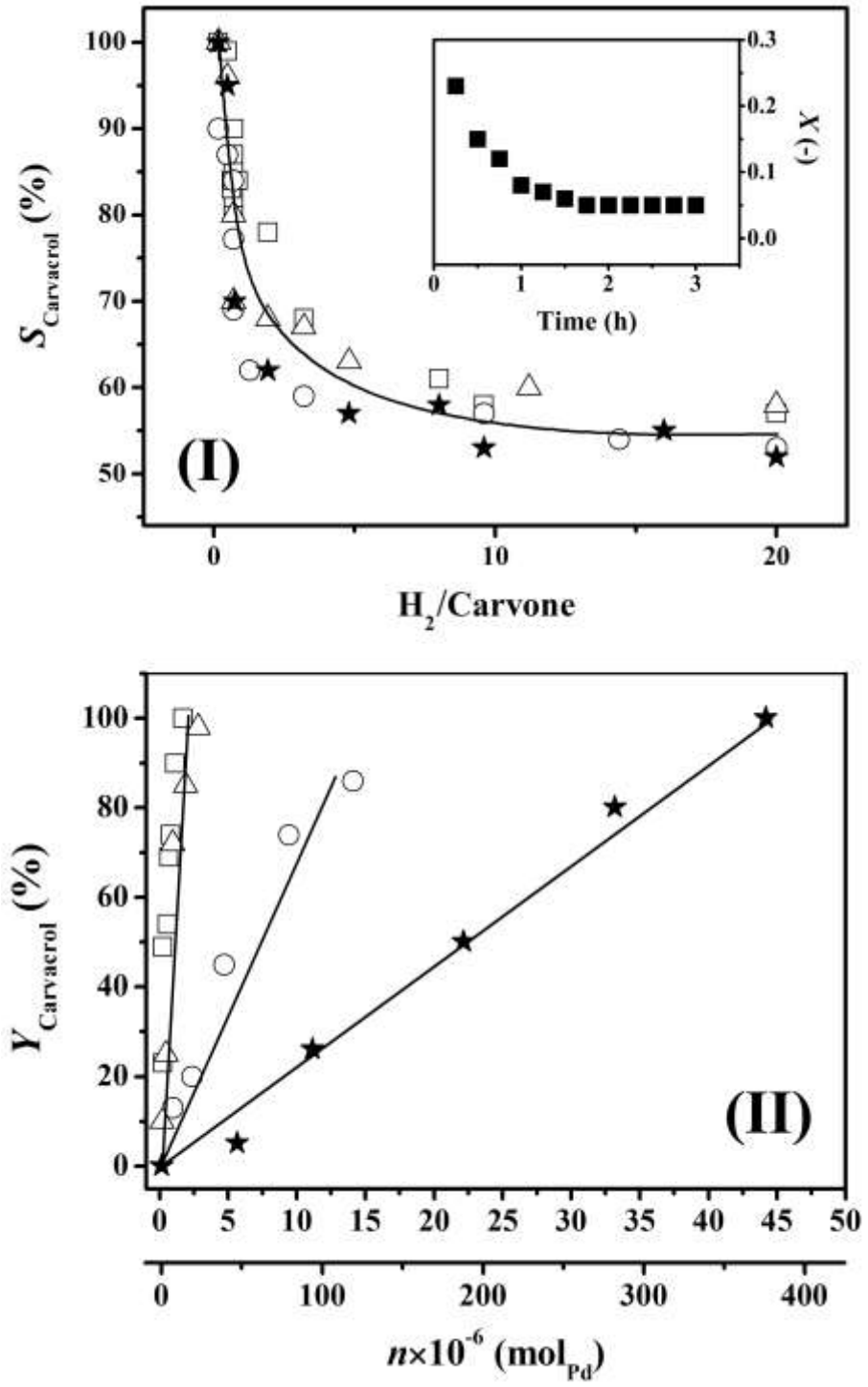
(I)
$S_{Carvacrol}$ (%)
H_2/Carvone
X (-)
Time (h)
(II)
$Y_{Carvacrol}$ (%)
$n\times10^{-6}$ (mol_{Pd})